AIP | Review of Scientific Instruments

An 8-GW long-pulse generator based on Tesla transformer and pulse forming network

Jiancang Su, Xibo Zhang, Rui Li, Liang Zhao, Xu Sun, Limin Wang, Bo Zeng, Jie Cheng, Ying Wang, Jianchang Peng, and Xiaoxin Song

Citation: Review of Scientific Instruments **85**, 063303 (2014); doi: 10.1063/1.4884341
View online: http://dx.doi.org/10.1063/1.4884341
View Table of Contents: http://scitation.aip.org/content/aip/journal/rsi/85/6?ver=pdfcov
Published by the AIP Publishing

An 8-GW long-pulse generator based on Tesla transformer and pulse forming network

Jiancang Su, Xibo Zhang, Rui Li, Liang Zhao,[a] Xu Sun, Limin Wang, Bo Zeng, Jie Cheng, Ying Wang, Jianchang Peng, and Xiaoxin Song
Science and Technology on High Power Microwave Laboratory, Northwest Institute of Nuclear Technology, Xi'an, Shaanxi 710024, China

(Received 31 March 2014; accepted 8 June 2014; published online 26 June 2014)

A long-pulse generator TPG700L based on a Tesla transformer and a series pulse forming network (PFN) is constructed to generate intense electron beams for the purpose of high power microwave (HPM) generation. The TPG700L mainly consists of a 12-stage PFN, a built-in Tesla transformer in a pulse forming line, a three-electrode gas switch, a transmission line with a trigger, and a load. The Tesla transformer and the compact PFN are the key technologies for the development of the TPG700L. This generator can output electrical pulses with a width as long as 200 ns at a level of 8 GW and a repetition rate of 50 Hz. When used to drive a relative backward wave oscillator for HPM generation, the electrical pulse width is about 100 ns on a voltage level of 520 kV. Factors affecting the pulse waveform of the TPG700L are also discussed. At present, the TPG700L performs well for long-pulse HPM generation in our laboratory. © *2014 AIP Publishing LLC*. [http://dx.doi.org/10.1063/1.4884341]

I. INTRODUCTION

Long-pulse generators are the foundation for generating high power microwaves (HPM) with a long pulse width.[1,2] In order to develop the long-pulse HPM technology, generators are required to deliver electric pulses with a width longer than 100 ns and an amplitude of about several hundred kilovoltages (kV).

Currently, it is feasible to build high-voltage long-pulse generators using a coaxial line as the pulse forming line (PFL). However, PFL would be too long if the pulse width exceeds 100 ns and if the coaxial lines are filled with gas or transformer oil. To solve this problem, spiral forming lines insulated by transformer oil were put forward.[3] This method can solve the problem to a certain extent, but the energy density of the PFL is not enhanced much. Afterwards, the de-ionized water and de-ionized water mixed with ethylene glycol which are of higher relative permittivity were introduced.[4,5] However, the characteristic impedance of a PFL insulated by de-ionized water usually mismatches that of an HPM load (~100 Ω). Therefore, improvements on the PFL are still needed. It is found that ceramics is a promising energy storing material. The reason lies in that ceramics has both the advantages of high dielectric constant and high dielectric breakdown strength. According to the following formula:

$$w = \frac{1}{2}\varepsilon_0 \varepsilon_r E_b^2, \tag{1}$$

where w is the energy density, ε_0 the dielectric constant in vacuum, ε_r the relative dielectric constant, and E_b the dielectric breakdown strength, a ceramic capacitor would have an energy density much higher than that of gas or liquid. When a number of ceramic capacitors are connected together with a special topological structure, they form a pulse forming network (PFN).[6] A PFN-based ceramic capacitor used as the energy storing unit has the advantages of compact structure, high operating voltage, and adjustable time delay.

Long pulse generators based on PFN were designed and studied by researchers. The typical generators include the PFN-Marx generators,[7,8] the linear transformer devices (LTD),[9–12] and the Tesla type generators (Tesla-PFN generators).[13–15] In the PFN-Marx type generators, all the PFN "behave" as a lumped capacitor when they are charged in parallel and as "a line" when discharge to a load. The PFN-Marx type generators can be constructed compactly. This is because a PFL is usually not needed in this type of generators. However, the PFN-Marx type generators have the disadvantages like low reliability since many gas switches are employed in the generators. In the LTD type pulse generators, a series PFN is used as the energy storage unit and the pulse forming modules simultaneously. The series PFN is connected to their respective primary sides of the generator via a lot of switches. When all the switches are triggered synchronously, the energy could be transferred from the PFN to a common secondary side via a 1:1 pulse transformer. If the synchronous precision of the switches is high and the performance of pulse transformer is stable, the pulses on the secondary side can overlap each other and can form a high-voltage pulse with an amplitude several times of the voltage amplitude on the primary side. However, when the synchronous precision of switches is low or the performance of the pulse transformer is unstable, pulse waveform on the secondary side of the transformer would be "bad". Aside from the two types, generators based on PFN and Tesla transformers are also put forward. Different from the PFN-Marx and the LTD, only one main switch is used in the Tesla-PFN type generators and all the PFN are charged by a Tesla transformer. So, the PFN-Tesla type generator has a higher reliability. A

[a]Author to whom correspondence should be addressed. Electronic mail: zhaoliang0526@163.com. Tel.: +86-29-84767631.

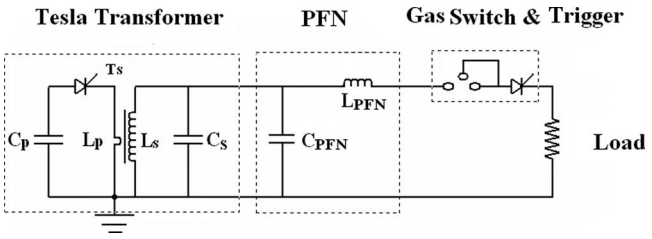

FIG. 1. Equivalent circuit of the TPG700L. C_p, C_s – the primary and the secondary capacitors of the Tesla transformer (TT); L_p, Ls – the primary and the secondary inductors of TT; Ts – the thyristor of TT; C_{PFN}, L_{PFN} – the equivalent capacitor and the inductor of PFN.

prototype based on a Tesla transformer and a series of PFN was introduced in Ref. 13. This generator can output a pulse with a width of 100 ns and a maximum power of 5 GW.

In this paper, a long pulse generator TPG700L based on a series of PFN and a Tesla transformer is presented. This generator is capable of outputting pulses with a width of 200 ns and a power of about 8 GW. The basic principle of this generator is introduced in Sec. II. The key components of the TPG700L are explained in Sec. III. In Sec. IV, the test results on a water load and a relative backward wave oscillator (RBWO) are introduced. Sec. V is the summary in this paper.

II. PRINCIPLE OF TPG700L

Fig. 1 shows the equivalent circuit of the TPG700L, in which four sub-circuits are included: the equivalent circuit of the Tesla transformer,[16–19] the equivalent circuit of the PFN, the circuit for the gas switch and the trigger, and the circuit of the load. Based on this circuit, the functioning process of the TPG700L can be described as follows: (1) the primary capacitor (C_p) of the Tesla transformer (TT) is charged by a DC power supply to a certain value within tens of milliseconds (ms); (2) the thyristor (T_s) is triggered and a high-voltage pulse with an amplitude greater than 1 MV is imposed on the second capacitor (C_s) due to the resonant effect of the TT (mainly from the loop of L_pC_p to L_sC_s), and simultaneously, the capacitor of the PFN (C_{PFN}) is charged to the same voltage of C_s; (3) when the gas switch is triggered by an external signal, the energy stored in C_s and C_{PFN} is delivered to the Load, and a pulse with a width of several hundred ns is formed.

For the TPG700L, the DC power can charge C_p to 800 V within 10–20 ms. When T_s is triggered, the voltage on C_s and C_{PFN} can be boosted to 1.2 MV. After the main switch is triggered, a 200-ns high-voltage pulse with amplitude of about 550∼600 kV is imposed on the load. If the impedance of the load matches that of the transmission line (TL) (40 Ω), then the power (P) of the TPG700L can be calculated as follows:

$$P = \frac{U^2}{Z}, \tag{2}$$

where U is the voltage on the load, Z the impedance of the load. As a result, the output power of the TPG700L is about 8 GW.

III. KEY COMPONENTS OF TPG700L

Fig. 2 shows the schematic diagram of the TPG700L. This diagram not only includes the aforementioned components like the PFN, the Tesla Transformer (built in a PFL), the gas gap switch, the trigger (built in a TL), and the load (the foilless diode),[20] but also includes two DC power supply and one control unit. The PFN component is accommodated in a cylindrical container which is connected to the left side of the PFL. Both the PFL and the PFN are charged by the Tesla transformer. The gas gap switch is connected to the right side of the PFL. The TL is assembled between the gas gap switch and the load in order to transmit the high-voltage pulse to the load with fidelity. The two DC power supplies are used to supply energy to the Tesla transformer and the trigger, respectively. The control unit is used to give off external signals to the two power supplies. The design considerations for key components are introduced in detail in Secs. III A–III E.

A. PFN

The PFN is composed of 12 stages of PFN modules. These modules are also named capacitor-loaded lines. For each capacitor-loaded line, it comprises two flat plates and several high-voltage ceramic capacitors, and is fabricated to be a shape of "C", as shown in Fig. 3. The maximum operating voltage of the ceramic capacitors is 25 kV, and its

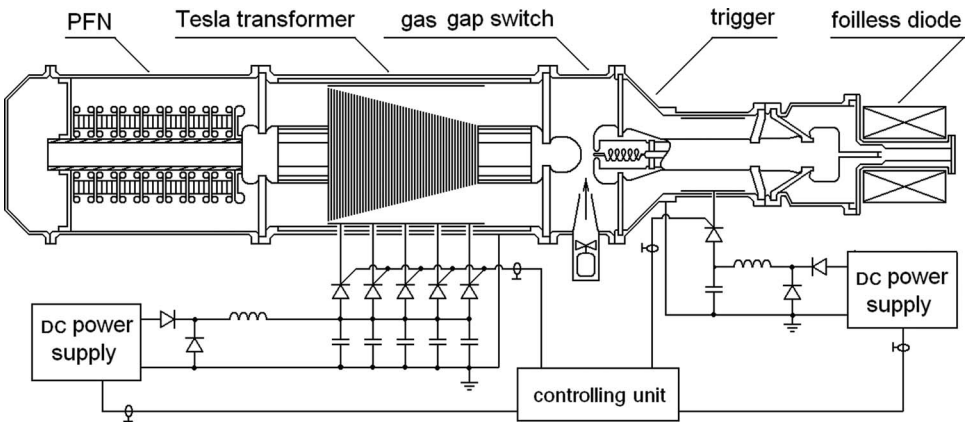

FIG. 2. Schematic diagram of the TPG700L.

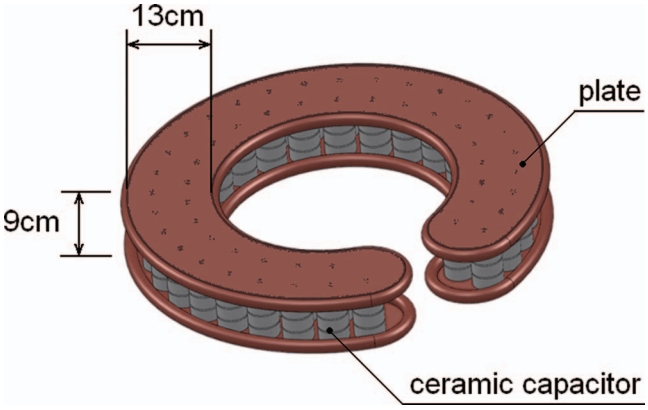

FIG. 3. Configuration of a capacitor-loaded line (one stage of PFN).

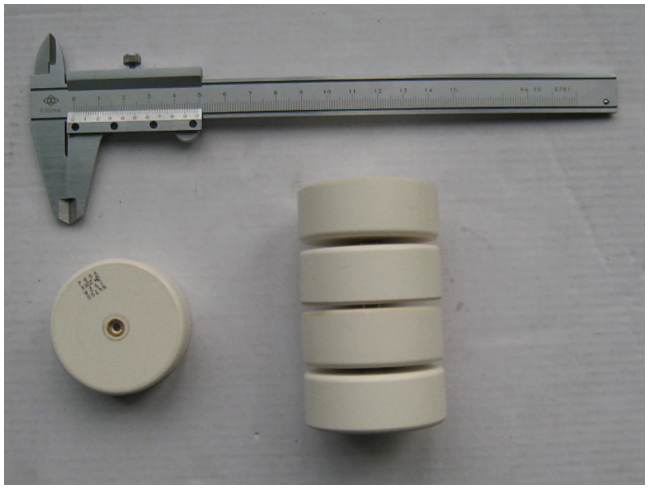

FIG. 4. Photo of a capacitor group.

capacitance is 2.5 nF. Four ceramic capacitors are connected in series to form a capacitor group, as shown in Fig. 4, and 32 capacitor groups connected in parallel are assembled between the two flat electrodes. Therefore, the maximum voltage and the capacitance of a loaded line are 100 kV (25 kV × 4) and 20 nF (2.5 nF ÷ 4 × 32), respectively. The inductance of a loaded line is designed to be 220 nH. So the impedance of a loaded line is 3.3 Ω according to the following formula:

$$Z_{PFN} = \sqrt{L_{PFN}/C_{PFN}}, \tag{3}$$

where Z_{PFN} is the impedance of the loaded line, L_{PFN} and C_{PFN} the inductance and capacitance of the loaded line, respectively. The width of the plate electrodes is 13 cm and the distance between the two electrodes is 9 cm. The plates are made of copper. The edges of the plate electrodes are welded to copper tubes with a diameter of 20 mm in order to reduce the edge electric field strength.

Since 12 stages of loaded lines are stringed in series to form a PFN, the maximum operating voltage of the PFN is about 1.2 MV (100 kV × 12), the impedance of the PFN is 40 Ω (3.3 Ω × 12), and the total capacitance is 1.67 nF (20 nF ÷ 12). The theoretical delay time of the PFN, t_{PFN}, can be calculated as follows:

$$t_{PFN} = Z_{PFN}\,(C_{PFN} + C_{st}), \tag{4}$$

where Z_{PFN} and C_{PFN} are as defined in (3), C_{st} the spray capacitance of the PFN, which is estimated to be 0.5 nF. With these values, t_{PFN} is calculated to be 87 nF. Fig. 5 shows the output pulse waveform of the loaded line. From this figure, it is seen that the pulse width is about 160 ns. This result is in line with the theoretical value, which is about two times of t_{PFN}. Fig. 5 also shows that the rise time of pulse is about 20 ns. The theoretical analysis shows that the rise time of the output pulse can be reduced effectively by using capacitors of

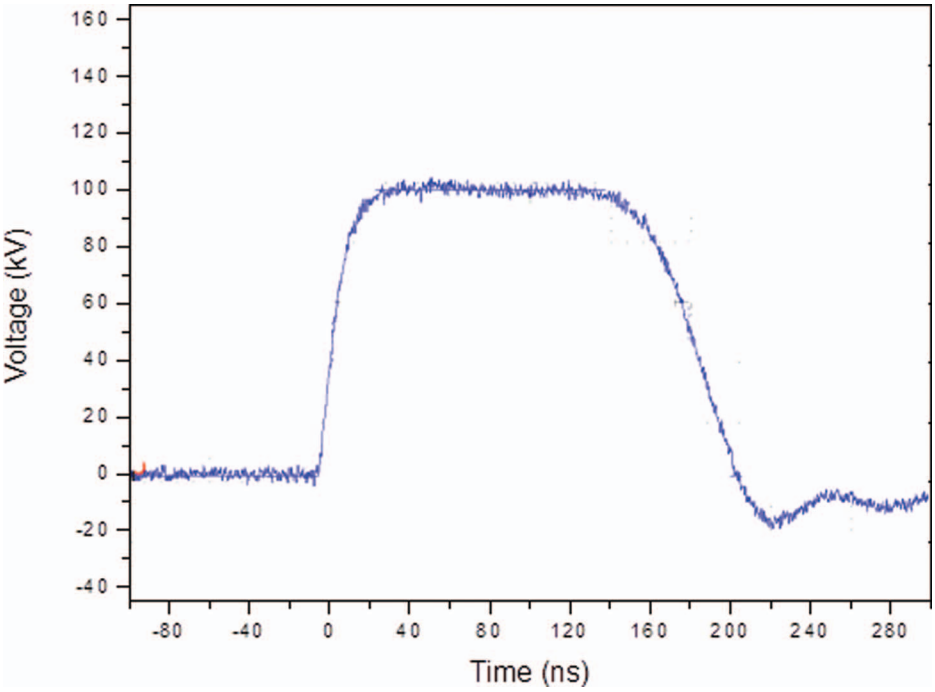

FIG. 5. Output voltage waveform of the capacitor-loaded line.

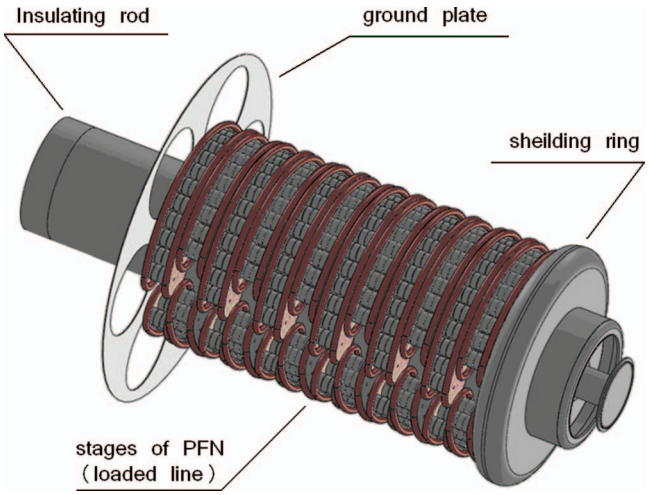

FIG. 6. 3D model of the series PFN.

small capacitance or by increasing the density of the capacitor groups between electrodes.

The PFN is assembled on an insulating cylinder, as show in Fig. 6. The first stage of the PFN is grounded; the 12th stage is connected to the inner conductor of the PFL via a shielding ring to obtain an electric field weaker than 180 kV/cm; the contiguous loaded lines of the PFN are insulated by the impregnated paper. The whole PFN is immersed in transformer oil to ensure global insulation.

B. Tesla transformer built in PFL

Fig. 7 shows the schematic of the Tesla transformer built in a PFL, which mainly comprises of a primary capacitor bank, dozens of thyristors, a one-turn primary winding coil, a 2500-turn secondary coil, and two open magnetic cores. The magnetic cores also serve as the inner and outer conductors of the PFL, which are separated by two PMMA (organic glass) plate insulators. The primary capacitor of the Tesla transformer is composed of 1000 metalized film capacitors with a total capacitance of 10 mF and a maximum charging voltage of 1200 V. A number of thyristors are paralleled to discharge to the primary coil synchronically. The primary and the secondary coils are built in the coaxial line, the length of which is 3.8 m. The surfaces of the inner and the outer conductors of the coaxial line are embedded with electrotechnical steel, which can enhance the coupling coefficient of the Tesla transformer up to 0.95. Because a recuperated diode is connected to the primary capacitor in parallel, the energy not resonant to the secondary loop can be recycled to the primary capacitor via this diode in each working period. Therefore, the energy loss is less than 20% and the energy efficiency of the Tesla transformer can exceed 70%.

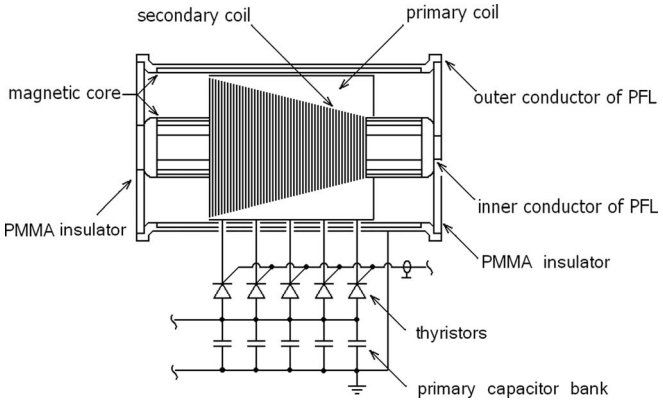

FIG. 7. Schematic diagram of the Tesla transformer built in PFL.

The characteristic impedance of the PFL is designed to be 40 Ω, using transformer oil as the insulating material. Since the charging process of the PFL can be finished in a 100 μs, this line can be equivalent to a part of the secondary capacitor of the Tesla transformer. When the PFL discharges to the load, it can be finished in tens of nanoseconds. Therefore, the PFL behaves as a "line", and it can form a short pulse on the load. The pulse width, τ_p, depends on the sum of the delay time of the PFL and PFN, which can be calculated as follows:

$$\tau_p = 2(t_{PFL} + t_{PFN}), \tag{5}$$

$$t_{PFL} = \frac{l_{PFL}\sqrt{\varepsilon_r}}{c}. \tag{6}$$

In (4) and (5), t_{PFL} and t_{PFN} represent the delay time of the PFL and PFN, respectively, c is the speed of light (3×10^8 m/s), l_{PFL} is the length of the PFL (3.8 m), and ε_r is the relative dielectric constant of transformer oil ($\varepsilon_r = 2.3$). With these parameters, t_{PFL} is calculated to be 19 ns. Since t_{PFN} is tested to be about 80 ns, τ_p is about 200 ns theoretically.

C. Gas gap switch

The TPG700L uses a gas gap as the main switch, which is shown in Fig. 8. The insulation gas is nitrogen (N_2). The gas pressure in the switch is in a range of 10–15 atm. A fan with a closed-loop pipeline is used to realize the gas circulation, which can blow high-temperature gas away from the discharging region and speed up the gas insulation recovery process after gas breakdown occurs. Aside from the cathode and the anode, there is also a third electrode, the triggered electrode. This triggered electrode is located at the axis of the switch. The trigger pulse is set to be positive, which is generated by a small Tesla transformer built in the TL. The voltage between the trigger electrode and the anode is about 10%–20% of the voltage between the cathode and the anode. The breakdown voltage of the main switch is set to be 90% of the charging voltage by setting the rise time of the waveform to

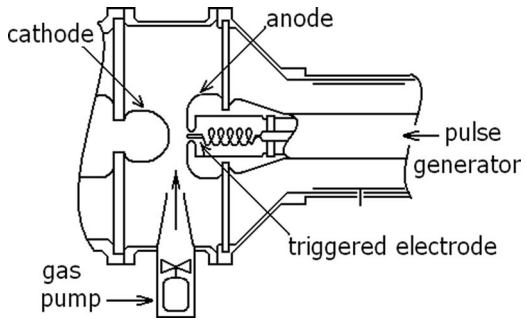

FIG. 8. Schematic diagram of the gas gap switch with a trigger.

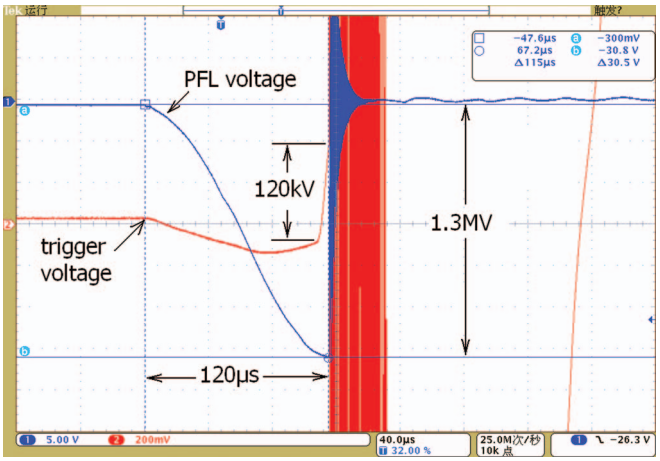

FIG. 9. Charging waveform on the PFL and the trigger waveform.

be 120 μs. Under the action of an over-voltage between the cathode and the trigger electrode, the gas breakdown in the switch takes place, and the switch is closed. The experimental results show that the TPG700L can operate at voltages up to 1.3 MV at a repetition rate of 50 Hz stably, as shown in Fig. 9.

D. Trigger built in the TL

As aforementioned, the trigger is built in the TL. The TL is also a coaxial line, the length of which is 2 m. One side of the TL is connected to the gas gap switch and the other connected to the load. The space between the inner and the outer conductors of the TL is filled with transformer oil to ensure insulation. The characteristic impedance of TL is 40 Ω, which matches that of the PFL. As aforementioned, a small Tesla transformer is assembled into the interior of TL to generate a high-voltage pulse to trigger the main switch. This small Tesla-type generator also comprises two open-circuit magnetic cores, a primary coil and a secondary coil. The inner magnetic core is an independent rod which is assembled in the inner conductor of the TL; and the outer magnetic core is embedded into the inner surface of the outer conductor. Both the magnetic cores are of the same length as that of the TL (Fig. 10(a)). The inner conductor of the TL is a thin hollow metal cylinder with a slot along the axis. When a surge of high

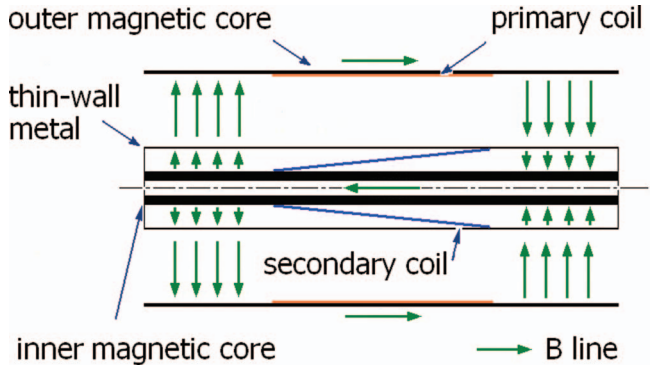

FIG. 10. Cross section of the triggered pulse generator built in TL.

FIG. 11. Global view of the TPG700L.

current flows through the primary coil which stuck to the outer magnetic core, the excited magnetic flux will pass through the thin hollow metal cylinder, which results in an induced electrodynamics' force on the secondary coil between the inner magnetic core and the thin-walled metal cylinder. Therefore, a trigger pulse is generated. It is worth mentioning that this method to generate a high-voltage pulse does not affect the transmission of the main pulse. In addition, the eddy current loss in the thin-walled metal cylinder is low. As a result, the energy efficiency of this small Tesla generator can reach 50%. A capacitive voltage divider is assembled in the interior of the TL's inner conductor to monitor the trigger pulse. The signal is educed via a segment of coaxial cable, which also plays the role of reducing the pre-pulse on the main switch.

E. Load

Two types of loads are designed for the TPG700L: a water load and a foilless diode. Each load is used to meet different application requirements, which is introduced in detail in Sec. IV.

The diameter of the TPG700L (including flange) is 1.2 m. The total length is 9 m. The series of PFN is 2.5 m in length, the PFL is 3.5 m in length, the gas gap switch is 0.5 m, the TL is 2 m, and the vacuum foilless diode is 0.5 m. The total weight of the TPG700L is about 15 tons. The global view of the TPG700L with the water load is shown in Fig. 11.

IV. EXPERIMENTAL RESULTS

A. Experimental results on water load

A water load with an impedance of 40 Ω is connected to the end of the TL, which is shown in Fig. 12. This load is used to test the output characteristics of the TPG700L. Approximately, this load can be considered as an extended part of the TL due to its matched impedance and absorption characteristics. The inner conductor of the load is a cylindrical thin water layer. The outer conductor is a metallic conical barrel, the radius of which gradually transits to that of the water layer. The input impedance of the absorption "TL" can be fixed to 40 Ω by regulating the conductivity of the water. The temperature increment of the water load caused by a pulse is less than 0.5 °C without considering the heat exchange. If the heat exchange is considered, the temperature increment would be much lower.

The envelope of the current pulse waveform of the TPG700L on the water load is shown in Fig. 13, which comprises 50 pulses at a repetition rate of 50 Hz. The amplitude

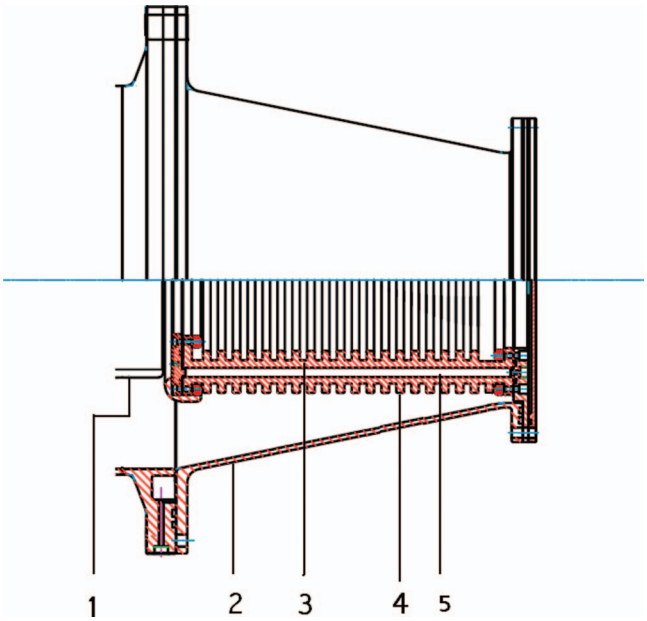

FIG. 12. Mechanical drawing of the water load. 1,2 – inner and outer conductors of the TL; 3,4 – inner and outer insulting layer of the water load; 5 – water layer.

of the current is over 15 kA, which is measured via a Rogowski coil. The output power is calculated to be over 8 GW ($P = I^2Z$). The full width at half maximum (FWHM) is tested to be larger than 200 ns; and the rise time is about 20 ns, which agrees with the theoretical design values.

It is noted that obvious oscillation exists on the top of the current waveform. The reasons for the "recess" can be understood in the following aspects: (1) Since the PFN is composed of capacitors, it has a finite maximum cut-off frequency, f_c. Whereas for the PFL, it is a coaxial line, and its maximum frequency is infinite. As a result, when a pulse transmits from the PFL to the PFN, the energy with a frequency higher than f_c would be reflected. These high-frequency spectra can add into the main waveform, which results in the oscillation. (2) The gas gap switch has a time-dependent impedance when gas breakdown occurs. This impedance is usually smaller than that of the PFL and the load. As a result,

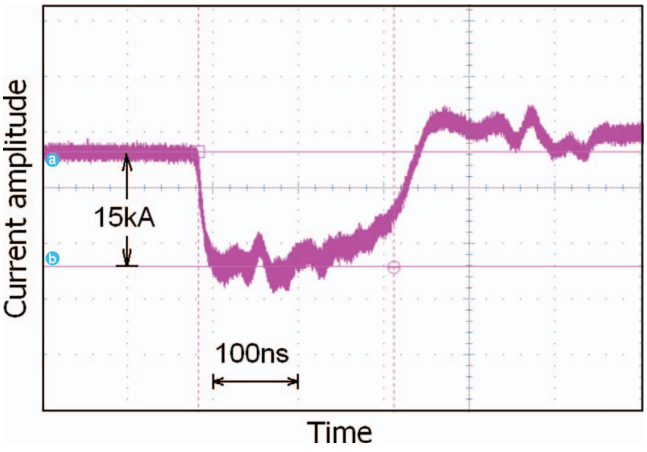

FIG. 13. Output current pulses into the water load.

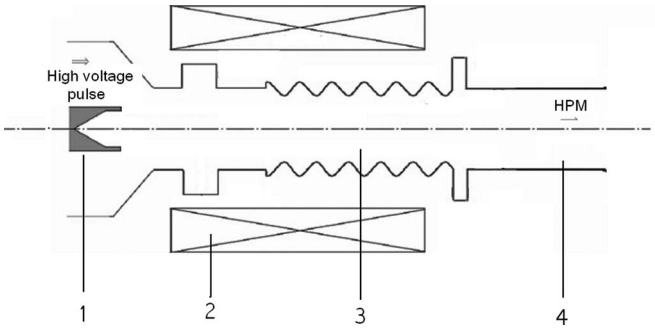

FIG. 14. Schematics of the RBWO. 1 – annular cathode; 2 – solenoid magnet; 3 – slow wave structure; 4 – waveguide.

when a pulse transmits from the PFL to the load, reflection from the switch can also add into the main waveform. (3) Furthermore, if the impedance of the load does not match that of the TL, the third reflection would be caused and added into the main waveform. In other words, in order to make the output waveform flat, the response ability of the PFN to the high-frequency spectra should be increased; the breakdown impedance of the gas gap switch should be decreased; and a matched impedance between the TL and the load should be designed.

B. Experimental results on BWO

Another important application of the TPG700L is to drive the long-pulse HPM, in which a RBWO is employed as the load, the schematics of which is shown in Fig. 14. More descriptions on RBWO can be seen in Refs. 21–25. Fig. 15 shows the envelope of the waveforms on the RBWO, in which the voltage and the current signals are measured via a capacitive voltage divider and a Rogowski coil, respectively. It can be seen from the figure that: (1) In the first 120 ns, the voltage waveform is quite similar to that of the current, which reveals that the impedance of RBWO is relatively stable after the electron beams were generated. From 120 ns to 160 ns, the current amplitude decreases slightly whereas the voltage amplitude decreases obviously. This means that the impedance of RBWO decreases somewhat. It is believed that this is

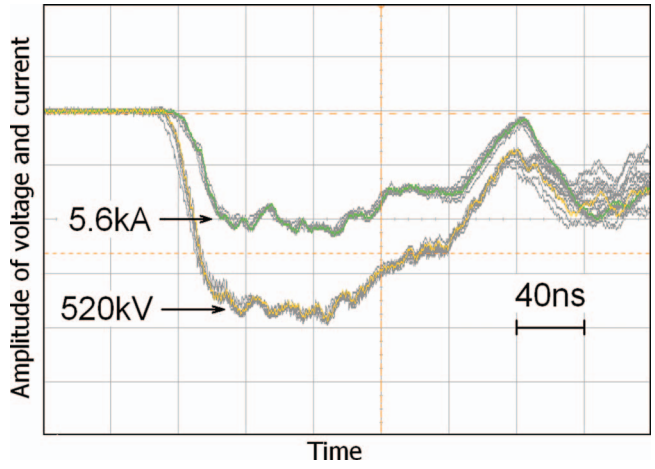

FIG. 15. Voltages and current waveforms on the RBWO.

related to the plasma formation process.[21–25] (2) The period of the small oscillations on the main pulse is about 20 ns. This corresponds to a length of 2 m, which is the length of the TL. The oscillation means that the impedances on both sides of the TL (switch and load) are mismatched. (3) The amplitude of the voltage and the current pulse both decrease obviously in the last 80 ns. This is related to the impedance distribution of the series PFN. The characteristic impedance of the PFN can be affected by the electromagnetic coupling between different stages of the loaded lines and the distributed capacitance between the PFN and the cylindrical container. The coupling makes the whole series PFN behave as a lumped capacitor, rather than a line when discharging to the load. The disadvantage of coupling effect of the PFN can be decreased by adjusting the impedance distribution of a single stage of the loaded line.

V. SUMMARY

A long pulse generator capable of outputting pulses with a width of 200 ns and a power about 8 GW is presented. The experimental results on this generator prove the feasibility to construct generators outputting MV-class, 100-ns HV pulses via the Tesla transformer and the PFN technologies. This Tesla-PFN type of generators can be used to drive the RBWO to generate long-pulse HPM with a width longer than 100 ns. The output characteristics of the Tesla-PFN type of generators can be improved by increasing the energy density of the ceramic capacitors and the operating voltage. The response ability of the PFN to pulses with a shorter rise time can be further increased and the top flatness of the output pulses would be improved.

It is worth mentioning that configuration of the TPG700L is a little "large" even ceramics capacitors with high energy density are used. Currently, a long-pulse generator capable of producing higher power with much smaller size is planned to be constructed in our laboratory.

[1]J. Benford, J. A. Swegle, and E. Schamiloglu, *High Power Microwaves*, 2nd ed. (Taylor & Francis, New York, London, 2008).
[2]J. Zhang, Z. X. Jin, J. H. Yang, H. H. Zhong, T. Shu, J. D. Zhang, Bao Liang Qian, C. W. Yuan, Z. Q. Li, Y. W. Fan, S. Y. Zhou, and L. R. Xu, IEEE Trans. Plasma Sci. **39**(6), 1438 (2011).
[3]S. D. Korovin, V. P. Gubanov, A. V. Gunin, I. V. Peget, and A. S. Stepchenko, in *Proceedings of the 13th IEEE International Pulsed Power Conference* (Las Vegas, NV, 2001), Vol. 2, p. 1249.
[4]J. H. Yang, H. H. Zhong, T. Shu, J. D. Zhang, J. L. Liu, J. H. Feng, and X. Zhou, High Power Laser Part. Beams **17** (8), 1191 (2005) (in Chinese).
[5]Z. C. Zhang, J. D. Zhang, J. H. Yang, and X. Zhou, High Power Laser Part. Beams **17**(8), 1201 (2005) (in Chinese).
[6]H. Bluhm, *Pulsed Power Systems* (Springer, Karlsruhe, 2006).
[7]D. A. Phelps, in *Proceedings of the IEEE 19th Conference on Power Modulator Symposium* (IEEE, 1990), p. 507.
[8]M. M. Kekez, *Pulsed Power Plasma Science, Digest of Technical Papers* (IEEE, 2001), Vol. 2, p. 1027.
[9]B. M. Kovalchuk, A. A. Kim, E. V. Kumpjak, N. V. Zoi, and V. B. Zorin, *Pulsed Power Plasma Science, Digest of Technical Papers* (IEEE, 2001), Vol. 2, p. 1488.
[10]A. N. Bastrikov, A. A. Kim, B. M. Kovalchuk, and E. V. Kumpjak, in *Proceedings of the 11th IEEE International Pulsed Power Conference* (IEEE, 1997), Vol. 1, p. 489.
[11]A. A. Kim, A. N. Bastrikov, S. N. Volkov, V. G. Durakov, B. M. Kovalchuck, and V. A. Sinebryukhov, in *Proceedings of the 14th IEEE International Pulsed Power Conference* (IEEE, 2003), Vol. 2, p. 853.
[12]J. J. Ramirez, K. R. Prestwich, and I. D. Smith, Proc. IEEE **80**, 946–957 (1992).
[13]J. C. Su, X. B. Zhang, G. Z. Liu, X. X. Song, Y. F. Pan, L. M. Wang, J. C. Peng, and Z. J. Ding, IEEE Trans. Plasma Sci. **37**(10), 1954 (2009).
[14]X. B. Zhang, J. C. Su, L. M. Wang, Y. F. Pan, Z. J. Ding, and L. Zhao, High Power Laser Part. Beams **21**(4), 591 (2009) (in Chinese).
[15]R. Li, X. B. Zhang, J. C. Su, J. C. Peng, W. H. Guo, and L. M. Wang, High Power Laser Part. Beams **23**(11), 2893–2896 (2011) (in Chinese).
[16]L. Zhao, G. Z. Liu, J. C. Su, Y. F. Pan, and X. B. Zhang, IEEE Trans. Plasma Sci. **39**(7), 1613–1618 (2011).
[17]L. Zhao, Y. F. Pan, J. C. Su, X. B. Zhang, L. M. Wang, J. P. Fang, X. Sun, and R. Lui, Rev. Sci. Instrum. **84**, 105114 (2013).
[18]B. M. Novac, R. Kumar, and I. R. Smith, Rev. Sci. Instrum. **81**(10), 104704 (2010).
[19]J. C. Peng, G. Z. Liu, X. X. Song, and J. C. Su, Laser Part. Beams **29**(1), 55 (2011).
[20]S. Huo, C. Chen, J. Sun, Z. Song, R. Xiao, W. Song, and Y. Teng, IEEE Trans. Plasma Sci. **41** (10), 2763 (2013).
[21]Y. Teng, R. Z. Xiao, Z. M. Song, S. Jun, C. H. Chen, H. Shao, G. Z. Liu, and C. X. Tang, Rev. Sci. Instrum. **82**(2), 024701 (2011).
[22]W. Song, X. W. Zhang, C. H. Chen, J. Sun, and Z. M. Song, IEEE Trans. Electron Devices **60**(1), 494–497 (2013).
[23]R. Z. Xiao, X. W. Zhang, L. J. Zhang, X. Z. Li, L. G. Zhang, W. Song, Y. M. Hu, J. Sun, S. F. Huo, C. H. Chen, Q. Y. Zhang, and G. Z. Liu, Laser Part. Beams **28**(3), 505 (2010).
[24]S. D. Korovin, V. V. Rostov, S. D. Polevin, I. V. Pegel, E. Schamiloglu, M. I. Fuks, and R. J. Barker, Proc. IEEE **92**(7), 1082 (2004).
[25]X. X. Song, G. Z. Liu, J. C. Peng, J. C. Su, L. M. Wang, X. X. Zhu, P. Y. Feng, X. B. Zhang, W. H. Guo, S. Qiu, and W. H. Huang, in *Proceedings of the 17th International Conference on High-Power Particle Beams*, Xi'an China (IEEE, 2008), p. 75.